Organization of pp60^{src} and Selected Cytoskeletal Proteins within Adhesion Plaques and Junctions of Rous Sarcoma Virus-transformed Rat Cells

KATHY SHRIVER and LARRY ROHRSCHNEIDER
Fred Hutchinson Cancer Research Center, Seattle, Washington 98104

ABSTRACT The localization of pp60^{src} within adhesion structures of epithelioid rat kidney cells transformed by the Schmidt-Ruppin strain of Rous sarcoma virus was compared to the organization of actin, α-actinin, vinculin (a 130,000-dalton protein), tubulin, and the 58,000-dalton intermediate filament protein. The adhesion structures included both adhesion plaques and previously uncharacterized adhesive regions formed at cell-cell junctions. We have termed these latter structures "adhesion junctions." Both adhesion plaques and adhesion junctions were identified by interference-reflection microscopy and compared to the location of pp60^{src} and the various cytoskeletal proteins by double fluorescence. The results demonstrated that the *src* gene product was found within both adhesion plaques and adhesion junctions. In addition, actin, α-actinin, and vinculin were also localized within the same pp60^{src}-containing adhesion structures. In contrast, tubulin and the 58,000-dalton intermediate filament protein were not associated with either adhesion plaques or adhesion junctions.

Both adhesion plaques and adhesion junctions were isolated as substratum-bound structures and characterized by scanning electron microscopy. Immunofluorescence revealed that pp60^{src}, actin, α-actinin, and vinculin were organized within specific regions of the adhesion junctions. Heavy accumulations of actin and α-actinin were found on both sides of the junctions with a narrow gap of unstained material at the midline, whereas pp60^{src} stain was more intense in this central region. Antibody to vinculin stained double narrow lines defining the periphery of the junctional complexes but was excluded from the intervening region. In addition, the distribution of vinculin relative to pp60^{src} within adhesion plaques suggested an inverse relationship between the presence of these two proteins.

Overall, these results establish a close link between the *src* gene product and components of the cytoskeleton and implicate the adhesion plaques and adhesion junctions in the mechanism of Rous sarcoma virus-induced transformation.

Infection of susceptible chicken and mammalian cells with Rous sarcoma virus (RSV) leads to the genetically controlled expression of viral functions and the transformation of these cells to the neoplastic state. This transforming event is mediated by a single genetic locus within the viral genome called the *src* gene (46). The product of the *src* gene is a 60,000-dalton phosphoprotein (pp60^{src}; 3, 29, 34, 39) possessing a unique kinase activity capable of phosphorylating substrate proteins on tyrosine residues (21). Because of this enzymatic activity, transformation in this system has been proposed to involve phosphorylation of host cell proteins (8, 21), and recent evidence has indicated that RSV-transformed cells possess elevated levels of phosphotyrosine in host cell proteins (40). Clearly, locating the intracellular target site(s) of pp60^{src} is of importance in understanding the mechanism of transformation, for the study of these sites may lead to the identification of one or more phosphotyrosine-containing substrate proteins.

Several diverse locations of pp60^{src} within RSV-transformed cells have been reported. Initial immunofluorescence experiments indicated that, in contrast to the early finding of the nuclear location of the papova virus large T-antigens (33), the RSV *src* gene product was situated within the cytoplasm of RSV-transformed cells (4, 35, 50). The latter studies also demonstrated other locations of pp60^{src} within the cytoplasmic

THE JOURNAL OF CELL BIOLOGY · VOLUME 89 JUNE 1981 525-535

compartment. pp60^{src} was found in a subcytoplasmic concentration in the perinuclear region (35) and concentrated on the cytoplasmic side of cell-cell junctions (35, 50). The plasma membrane, as well as other intracellular membranes, also have been found to harbor a high percentage of pp60^{src} presumably attached by some means to the cytoplasmic face of the membranes (10, 25, 26, 50).

In addition to these locations, we recently presented evidence (37) that pp60^{src} was associated with the adhesion plaques of RSV-transformed cells. The adhesion plaques are components of the cytoskeleton where microfilament bundles terminate and anchor the plasma membrane to the substratum (1, 19, 23). Therefore, pp60^{src} at these sites is directly associated with the cytoskeleton. This was also suggested by the studies of Burr et al. (6), who found an enzymatically active pp60^{src} in cytoskeletons prepared from RSV-transformed cells.

The interaction of pp60^{src} with adhesion plaque structures has the potential for explaining many properties of RSV-transformed cells. Certainly, the rapid dissolution of cytoskeletal microfilament bundles is one property that could be affected by pp60^{src} at these loci. We examine here the relationship of the cytoskeletal proteins actin, α-actinin, tubulin, intermediate filament protein, and vinculin (a 130,000-dalton protein of adhesion plaques) to the organization of pp60^{src} within the adhesion plaques and cell-cell junctions.

MATERIALS AND METHODS

Cells and Viruses

Normal rat kidney (NRK) cells were from a described epithelioid clone (36). A line of NRK cells transformed with the Schmidt-Ruppin Strain of Rous sarcoma virus subgroup D (SR-RSV-D), designated SR-NRK clone A4B5, was isolated by growth in methylcellulose and again by end-point dilution. The transformed cell line used in this study (SR-NRK-A4B5G4) was obtained by further recloning. All cells were cultured in Eagle's Minimal Essential Medium plus 10% calf serum. The cell lines were tested by staining with 4,6-diamidino-2-phenylindole (DAPI) and found negative for Mycoplasma contamination.

Antigen Preparation

Vinculin and α-actinin were prepared by the method of Geiger (16). Briefly, chicken gizzard muscle was homogenized and extracted according to the protocol of Singh et al. (43). A pellet of myofibril proteins was obtained by precipitating the pooled, deionized water extracts with 30% saturated ammonium sulfate. The pellet, which was dissolved in 20 mM tris-acetate, pH 7.5, and dialyzed, contained filamin, vinculin, α-actinin, desmin, and actin, as well as many unidentified minor proteins. This crude fraction was used for further purification of vinculin and α-actinin, and was also used for the preabsorption experiments described in the Immunofluorescence Microscopy section below. Vinculin and α-actinin were further purified by chromatography on a DEAE-cellulose column, as described by Geiger (16). Vinculin was then dialyzed against phosphate-buffered saline (PBS) and used for antibody production. α-Actinin was electroeluted from an SDS-polyacrylamide preparative gel before its use as an antigen.

Neurotubulin was prepared from 20-d-old chick embryo brain tissue by the thermal cycling method of Weisenberg (49) as modified by addition of glycerol (41). Microtubule-associated proteins were separated from tubulin by phosphocellulose chromatography (51). As a final purification step, tubulin was electroeluted from an SDS-polyacrylamide preparative gel.

Immune Reagents

Antitumor serum was prepared in New Zealand rabbits by the method of Brugge and Erikson (3), as described previously (35). Antitumor serum from marmosets was obtained from Fritz Deinhardt (Max von Pettenkofer-Institut für Hygiene und Medizinische Mikrobiologie der Ludwig-Maximilians-Universtät München) and is similar to that described by Brugge et al. (5). Immunoprecipitation of pp60^{src} by this serum has been described (38). Rabbit antiactin IgG was a gift from Patricia Maness (University of North Carolina). Rabbit antibodies to the 58,000-dalton subunit of the 10-nm intermediate filaments of cultured fibroblasts were obtained from Richard Hynes (Center for Cancer Research, Massachusetts Institute of Technology).

Antiserum against vinculin was prepared in a guinea pig by injections at multiple subcutaneous sites with 270 μg of purified protein in complete Freund's adjuvant, followed by a boost of 150 μg of protein in incomplete Freund's adjuvant after 3 wk. The animal was boosted once again after 2 more wk, and the serum was taken 1 wk later. A similar injection schedule was used for production of guinea pig antitubulin serum, the initial injection containing 2.0 mg of protein, followed by two booster injections of 1.0 mg each. Rabbit anti-α-actinin serum was prepared by an initial injection of 400 μg of protein, followed by three boosts of 200 μg each. Active antisera were identified by the appearance of precipitin lines in an immunodiffusion test with purified, electroeluted proteins. Antitubulin and anti-α-actinin were purified by affinity chromatography (44). The background fluorescence produced by the guinea pig antivinculin serum in NRK and SR-NRK cells was so low that affinity purification was not necessary. Antisera against tubulin and vinculin specifically precipitated the corresponding antigens from [^{35}S]methionine-labeled lysates of SR-NRK cells (not shown). Specificity of the antiserum against α-actinin, which did not readily precipitate the antigen, was demonstrated by radiographic detection of antibodies bound to extract proteins that had been separated by gel electrophoresis and transferred to nitrocellulose (data not shown).

All rhodamine- and fluorescein-conjugated antibodies were obtained from N. L. Cappel Laboratories Inc. (Cochranville, Pa.). Rhodamine-conjugated goat anti-rabbit IgG and fluorescein-conjugated goat anti-guinea pig IgG were affinity purified against the appropriate IgG fractions. Rhodamine-conjugated goat anti-human IgG (which cross reacted with marmoset IgG) and fluorescein-conjugated goat anti-rabbit IgG were absorbed in vivo in rats (35).

Immunofluorescence Microscopy

The immunofluorescence technique was similar to that described previously (35). Cells were seeded on ethanol-sterilized glass cover slips and allowed to grow for at least 2 d before use. Cells were fixed in 4% paraformaldehyde in PBS for 20 min, then permeabilized by treatment with 0.2% Triton X-100 in PBS for 3 min. After washing in PBS, each cover slip was then incubated with 40 μl of the first immune reagent in a humid chamber at 37°C. After 45 min, the cover slips were washed four times with PBS (5 min each), then incubated with 40 μl of the second immune reagent. In double localization experiments, rabbit antitumor serum was used in the first incubation when it was followed by guinea pig antivinculin or antitubulin reagents in the second incubation, and marmoset antitumor serum was used in the first incubation when it was followed by rabbit antiactin, anti-α-actinin, or anti-58,000-dalton reagents. The fluorescent reagents were allowed to bind in a third incubation at 37°C; combinations of either rhodamine-conjugated goat anti-rabbit IgG and fluorescein-conjugated goat anti-guinea pig IgG or rhodamine-conjugated goat anti-human IgG and fluorescein-conjugated goat anti-rabbit IgG were employed. Following the last incubation step, the cover slips were washed four times with PBS and mounted for interference-reflection microscopy (see below). For fluorescence visualization only, cover slips were mounted on a slide over a drop of PBS:glycerol (1:1) and sealed with Pro-Texx mounting medium (Scientific Products, Div. of American Hospital Supply Corp., McGaw Park, Ill.). Mounted cells were viewed with a Zeiss universal photomicroscope equipped with epi-illumination. Fluorescent images were recorded on Kodak Tri-X pan film rated at ASA 1000 and developed in Diafine (Acufine, Inc., Chicago, Ill.).

Affinity-purified antibodies (antitubulin, anti-α-actinin, and some fluorescent conjugates) were diluted in PBS to 50–100 μg/ml. Whole antisera and IgG fractions were diluted in heat-inactivated fetal calf serum, antitumor sera 1:30 (rabbit) or 1:40 (marmoset), antivinculin serum 1:30, and antiactin IgG to about 0.2 mg/ml. In addition, antitumor sera were absorbed just before use with 250 μg of SR-RSV-D, which was then removed by centrifugation. For the experiments shown in Fig. 3, diluted antitumor and antiactin sera were absorbed with 5 μg of chicken gizzard myofibril protein (described above) or with 20 mM tris-acetate buffer, pH 7.5, alone for 30 min at room temperature, then centrifuged before immunofluorescence.

Interference-Reflection Microscopy

Glass cover slips containing cells to be viewed by interference-reflection microscopy were mounted in PBS above 3-mm-deep glass chambers. The edges of the cover slips were sealed with Pro-Texx. The method of Curtis (11) was followed for setting the Zeiss Universal Photomicroscope for recording interference-reflection images, and the details have been described (37). Photographs were taken on Kodak Panatomic X film rated ASA 125 and developed in Kodak Microdol X.

Preparation of Adhesion Plaques

SR-NRK cells were plated on ethanol-sterilized glass cover slips and grown for 2 d before use. The cover slips were drained and washed in Dulbecco's modified PBS containing Ca^{2+} and Mg^{2+}. Each cover slip was extracted for 10 min on ice with 0.2% Triton X-100 in PBS (lacking Ca^{2+} and Mg^{2+}) containing trasylol (0.2 trypsin inhibitor units/ml). These conditions did not preserve intact microtubules. The cover slips were then washed briefly at room temperature with PBS and fixed for 20 min in 4% paraformaldehyde in PBS. After fixation, the cover slips were washed four times (5 min each) in PBS. Often the nuclei and cytoskeletons were washed off the glass cover slips during the PBS washes, leaving behind the adhesion plaques bound to the glass substratum. Residual nuclei and cytoskeletons were gingerly removed from the glass cover slip under a stream of PBS from a Pasteur pipet.

Scanning Electron Microscopy

Cellular material to be viewed by scanning electron microscopy was fixed in 1% glutaraldehyde in PBS for 60 min at room temperature, washed in PBS, and dehydrated stepwise in ethanol. After critical point drying using the freon method, the samples were coated with carbon and gold:palladium (60:40) by vacuum evaporation on a moving stage and viewed in a Cambridge Stereoscan Mark II electron microscope. The accelerating voltage was 22 kV.

RESULTS

Characterization of Antisera and Cytoskeletal Proteins in Normal Rat Cells

We performed immunofluorescence experiments with antisera to the cytoskeletal proteins actin, α-actinin, tubulin, intermediate filament protein, and vinculin to examine the distribution of these proteins in normal rat cells. We fixed the cells in paraformaldehyde and permeabilized them in Triton X-100, then incubated them with appropriately diluted antisera or affinity-purified antibodies, followed by a corresponding sec-

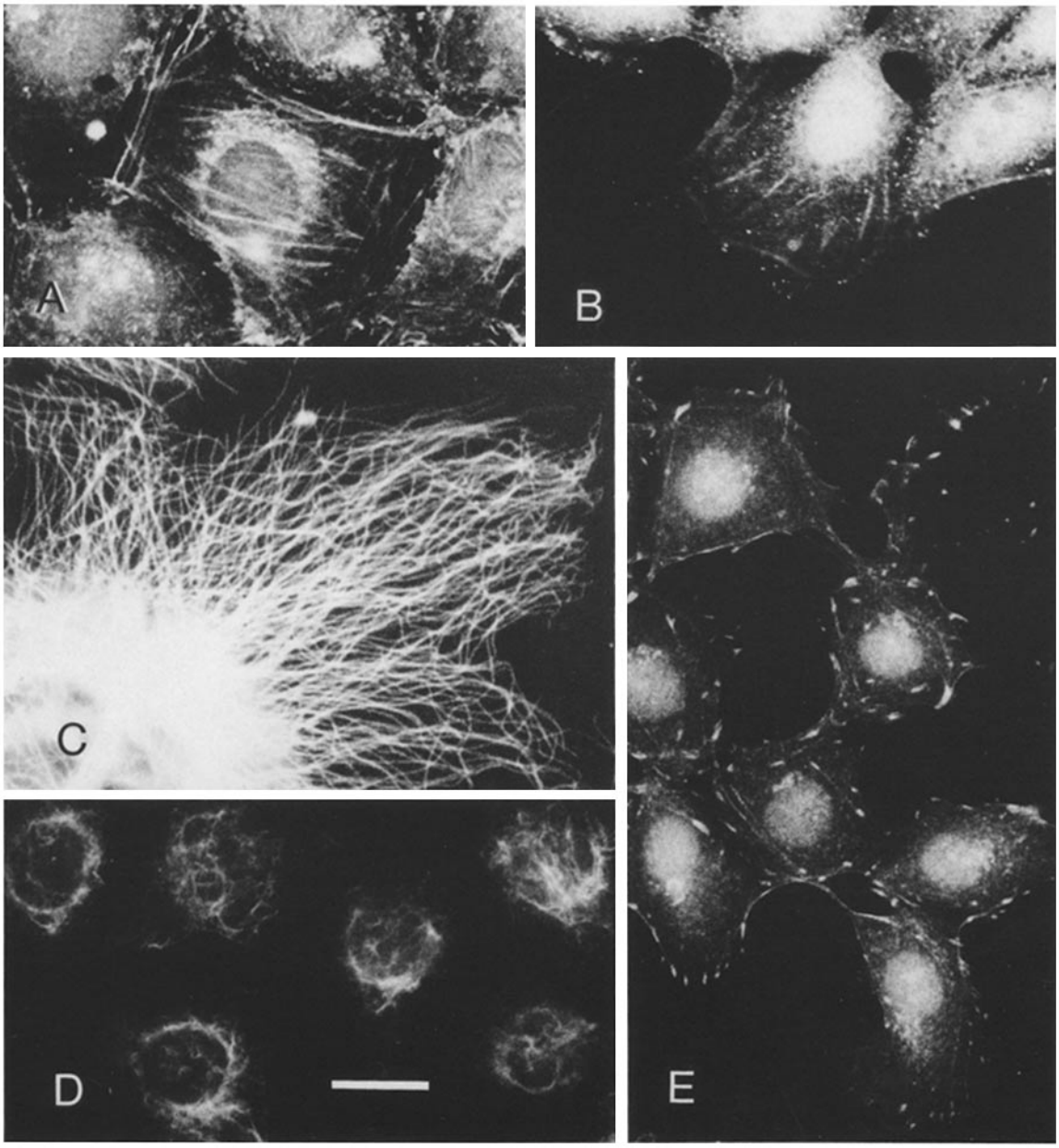

FIGURE 1 Demonstration of the specificity of various antisera to cytoskeletal proteins and the distribution of these proteins in uninfected NRK cells. NRK cells were fixed and stained by indirect immunofluorescence with antibodies to (*A*) actin, (*B*) α-actinin, (*C*) tubulin, (*D*) intermediate filament protein (58,000 daltons), and (*E*) a 130,000 dalton protein termed vinculin. Bar, 20 μm.

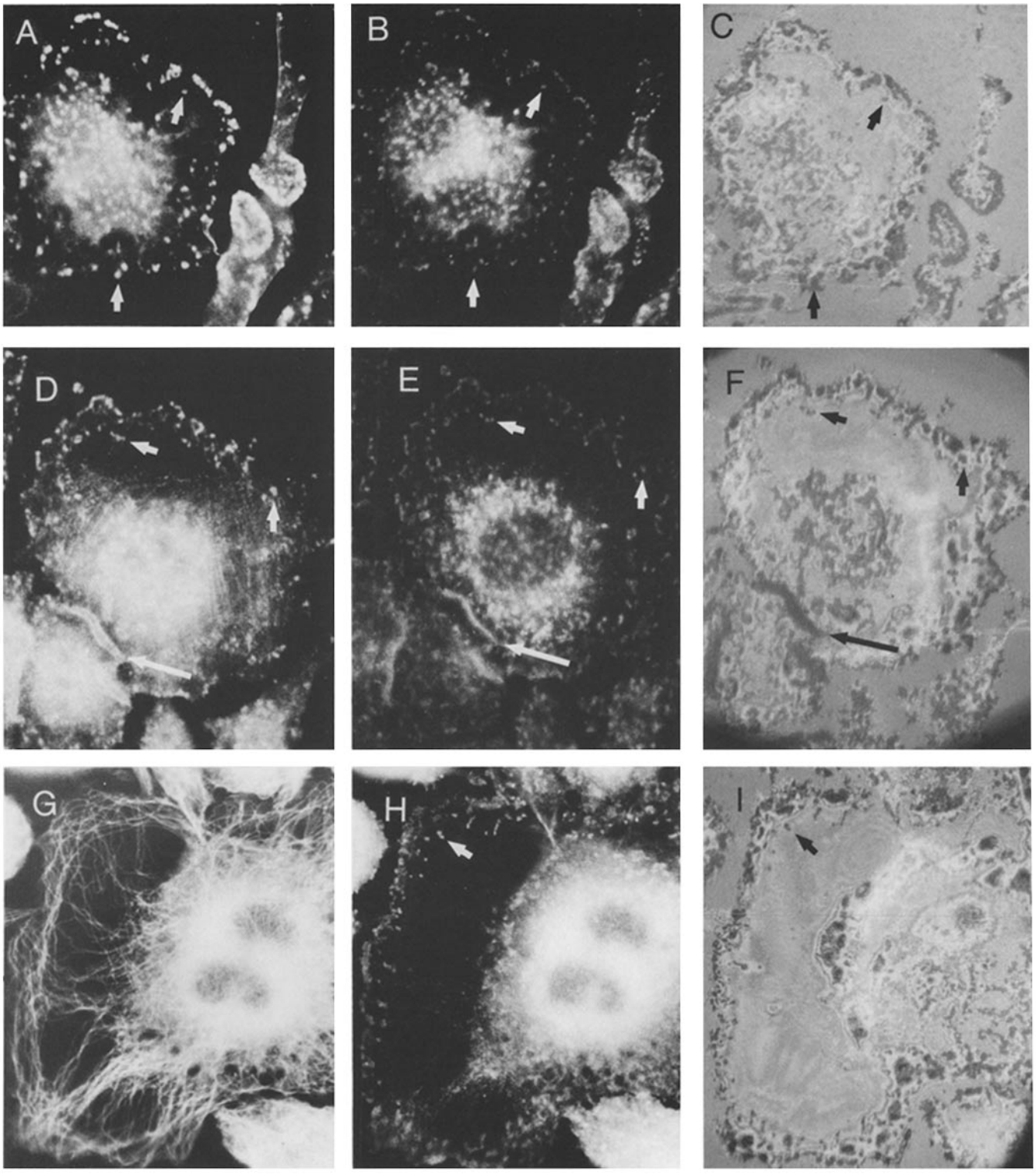

ond antibody conjugated to fluorescein or rhodamine. Actin antibody stained thick stress fibers that traversed the cell (Fig. 1 *A*). As expected, these fibers were organized either parallel to one another or converging at focal points (28). Ruffling edges were intensely stained, as were microspikes, particularly obvious in subconfluent cultures (not shown). Antibody against α-actinin stained the stress fibers weakly (Fig. 1 *B*). The same antiserum stained the stress fibers of normal rabbit fibroblasts (not shown) in a characteristic striated pattern (27). In the NRK cells, the fluorescence along the stress fibers was striated in some cases (27), but in general the stress fibers were not so prominent as when stained with antiserum to actin.

Antitubulin antibody stained an extremely well developed array of cortical microtubules in the interphase NRK cells (Fig. 1 *C*). The staining was such that individual microtubules could be easily traced from the perinuclear region to the cell periph-

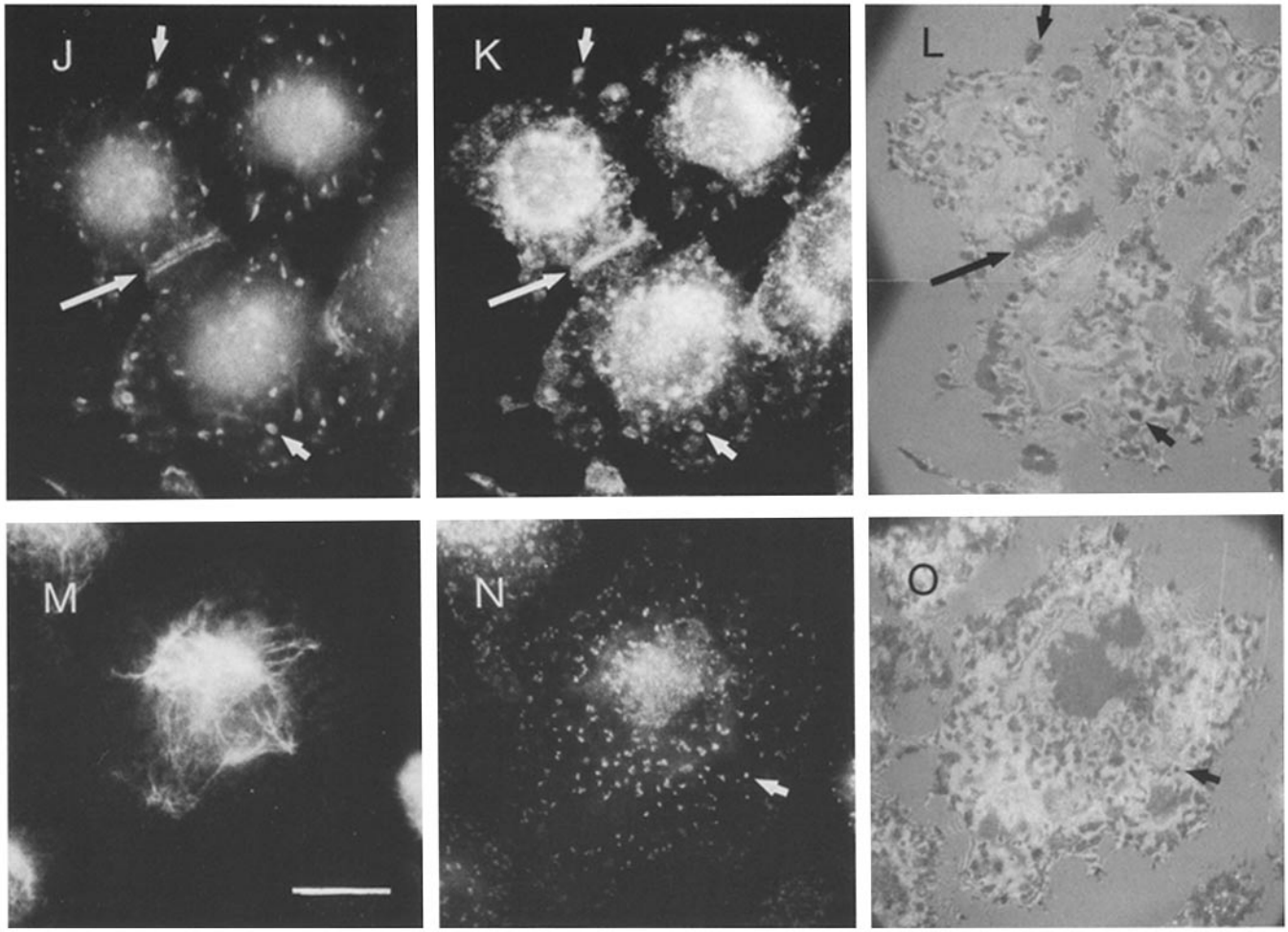

FIGURE 2 Simultaneous visualization of cytoskeletal proteins, pp60^{src}, and the cellular adhesion plaques of SR-NRK cells. SR-NRK cells were fixed and stained for double-chromophore indirect immunofluorescence using rabbit or guinea pig antibodies to the cytoskeletal proteins shown in Fig. 1 and the respective marmoset or rabbit antibodies to pp60^{src}. Appropriate combinations of fluoresceinated and rhodaminated antibodies were reacted with the first set of antibodies. To record these photographic images, the focal plane of the microscope was set near the ventral surface of a field of cells, and the fluorescence due to pp60^{src} and the respective cytoskeletal protein were recorded separately using appropriate filters. The adhesion plaques of the same field of cells were then recorded by interference-reflection microscopy. Each horizontal row of three photographs in this figure shows the same field of cells. (*A*) actin, (*B*) pp60^{src}, (*C*) adhesion plaques, (*D*) α-actinin, (*E*) pp60^{src}, (*F*) adhesion plaques, (*G*) tubulin, (*H*) pp60^{src}, (*I*) adhesion plaques, (*J*) vinculin, (*K*) pp60^{src}, (*L*) adhesion plaques, (*M*) 58,000 interediate filament protein, (*N*) pp60^{src}, (*O*) adhesion plaques. Short arrows point to prominent adhesion plaques, and long arrows point to junctions. Bar, 20 μm.

ery. Components of the mitotic spindle and midbody structures of dividing cells were also stained with antitubulin antibody (not shown). These staining patterns are typical of the distribution of tubulin within cells and have been described (15, 47).

Intermediate filaments within NRK wells were stained with antibodies to the 58,000-dalton subunit protein (22). This filament system was finer in structure and less abundant than the microtubules and appeared concentrated in the perinuclear region (Fig. 1 *D*). The intermediate filaments detected by this antiserum were clearly distinguishable from microtubules (14, 18, 22).

Vinculin, a 130,000-dalton protein originally isolated from smooth muscle, has been found at the ends of actin microfilament bundles coincident with the location of adhesion plaques in tissue culture cells (7, 16). The results in Fig. 1 *E* demonstrate the location of vinculin within NRK cells. As expected, small focal patches of fluorescence are seen near the ventral cell surface where adhesion plaques are found in these cells.

Simultaneous Observation of Cytoskeletal Proteins, pp60^{src}, and Adhesion Plaques in SR-NRK Cells

Having characterized the patterns of selected cytoskeletal proteins in normal cells, we then examined the effect of transformation by SR-RSV-D on these structures and the association of each with the transforming gene product. pp60^{src} was localized concurrently with the cytoskeletal proteins, using standard double-label immunofluorescence techniques. The adhesion plaques and areas of close cell contact with the substratum were viewed in these same fields of cells by interference-reflection microscopy.

Both rabbit antitumor serum (35) and marmoset antitumor serum (38) were employed to stain pp60^{src}. The staining patterns of both antisera were indistinguishable in all cells that we examined. In addition to staining in the perinuclear region and under the plasma membrane at areas of cell contact (35) both

sera revealed a distinct pattern of speckles at the ventral cell surface, a pattern that has been shown recently to coincide with the location of adhesion plaques in SR-NRK cells (37). This correspondence is readily apparent in Fig. 2. Observe that fluorescent speckles indicating the presence of pp60^{src} (Fig. 2 *B*, *E*, *H*, *K*, and *N*) match the dark focal contact points in interference-reflection micrographs of the same cells (Fig. 2 *C*, *F*, *I*, *L*, and *O*). In addition to the prominent focal adhesions observed at the cell perimeter, pp60^{src} often appeared in larger patches directly under the cell (e.g., Fig. 2 *N* and *O*). These areas probably correspond to close-contact areas (23).

A salient feature of those paired micrographs which displayed cell-cell contacts (e.g., Fig. 2 *E* and *F*, *K* and *L*) was the accumulation of pp60^{src} in a line at the interface between cells, a region which also featured a broad unbroken area of close contact with the substratum. We have termed these specialized regions "adhesion junctions." The formation of adhesion junctions appears to be a response to cell contact that is unique to the transformed cells, as such structures are never observed in confluent cultures of normal rat kidney cells.

The effect of transormation on actin distribution was dramatic. Instead of thick stress fibers, actin was localized in discrete patches, which appeared in a single focal plane at the ventral cell surface. These patches were either punctate, as in the large cell in Fig. 2 *A*, or coalesced to form scrolls as in the smaller cell at the right in Fig. 2 *A*. The distribution of actin within these RSV-transformed epithelioid NRK cells differed markedly from that reported previously for transformed fibroblasts (2, 12, 31, 45), and we attribute this to a species or cell type difference (see Discussion). It was immediately obvious that the array of actin staining in SR-NRK cells matched precisely the patterns of pp60^{src} stain, as well as the adhesion loci. A result similar to actin staining was observed when α-actinin was localized in SR-NRK cells. Although some cells retained a few fibers that stained in a striated fashion (Fig. 2 *D*), most cells exhibited only a pattern of ventral speckles that was coincident with pp60^{src} and the adhesion plaques. However, in contrast to the single band of pp60^{src} which appeared at the midline of adhesion junctions, both actin (not shown) and α-actinin (Fig. 2 *D*) staining of these junctions revealed a reciprocal pattern of two broad bands divided by a narrow central component that was unstained. The total width of this complex was equal to the width of the corresponding adhesion junction in an interference-reflection micrograph.

Microtubules in interphase SR-NRK cells were abundant (Fig. 2 *G*) and did not differ markedly from their normal counterparts, except that they were more difficult to photograph because the tumor cells were more rounded. There was no obvious association of microtubules with pp60^{src}-containing adhesion structures. Microtubules neither terminated at adhesion plaques nor appeared to associate with these structures in any obvious way. We did notice during the course of these studies (data not shown) that the location of the perinuclear spot stained by antitumor serum (35) coincided with the cytocenter for the organization of the microtubule network. The significance of this observation remains unknown.

Vinculin was localized in adhesion plaques in transformed cells (Fig. 2 *J*), but the morphology of these sites appeared altered. The vinculin loci in SR-NRK cells were punctate and stained with less intensity than the more elongated NRK "feet." Vinculin stained the adhesion junctions along two parallel lines separated by an unstained gap region. As before, pp60^{src} occupied the same junctions at the midline. A thorough comparison of vinculin and pp60^{src} in the adhesion plaques revealed differences in the intensity of certain loci. A number of "feet" which were uniformly stained for pp60^{src} were stained with variable intensities for vinculin, and some were virtually unstained (Fig. 2 *J* and *K*). (Possible consequences of such differences will be discussed subsequently.)

The distribution of the 58,000-dalton intermediate filament protein in SR-NRK, as revealed by immunofluorescence, did not differ markedly from that in NRK cells, except for those differences associated with a change in cell shape. We generally noted a paucity of intermediate filaments in both cell types when compared with the published fluorescence patterns of filaments in hamster cells (22). Again, we attribute this to a species and/or cell type difference. Intermediate filaments were not specifically associated with adhesion plaques or junctions (Fig. 2 *M–O*).

Reaction of Antitumor Serum with Adhesion Plaque pp60^{src} Is Not Blocked by Preabsorption with Cytoskeletal Proteins

Because the localization of pp60^{src} within the adhesion plaques of SR-NRK cells coincided so well with the distribution of actin and α-actinin in these cells, it was necessary to demonstrate clearly that autoantibodies in the antitumor serum were not responsible for this localization. Others have reported the presence of autoantibodies against cytoskeletal proteins in some preimmune rabbit sera (14, 18, 24). A priori, the evidence against a significant contribution by potential autoantibodies was overwhelming: (*a*) because anti-tumor serum did not stain any filamentous structures in NRK cells; and (*b*) because antitumor sera from different rabbits, as well as from a marmoset, gave identical staining of adhesion plaques.

Nevertheless, an immunofluorescence experiment was performed in which rabbit antitumor serum was first preabsorbed with a gizzard myofibril extract containing actin, α-actinin, filamin, desmin, and vinculin, as well as many unidentified proteins (see Materials and Methods). Preabsorption (Fig. 3 *b*) did not alter the number or intensity of pp60^{src} "feet" or adhesion junctions (not shown) relative to antitumor serum incubated with buffer alone (Fig. 3 *a*). However, preincubation of the antiactin serum with the same volume of myofibril extract clearly eliminated the specific staining of actin (Fig. 3 *c* and *d*). These results, along with previous studies (35), suggest that the antitumor serum is detecting only pp60^{src} within the adhesion plaques and junctions.

Identification of Cytoskeletal Proteins and pp60^{src} in Isolated Adhesion Plaques

We had noticed throughout these studies that cells that were inadvertently removed from the cover slips left behind a residue of material that stained with antitumor serum. We found that the removal of cells was facilitated by extraction with 0.2% Triton X-100 before fixation in paraformaldehyde. Cells were then washed away from the cover slips by blowing gently with a stream of buffer. Scanning electron microscopy of the material remaining on cover slips following this treatment revealed an array of globular units, which appeared analogous to the "feet," as well as heavier accumulations of material corresponding to the adhesion junctions (Fig. 4). Recalling that focal contacts in transformed NRK cells are not elongated, the size of these "feet" is in a range consistent with adhesion plaques

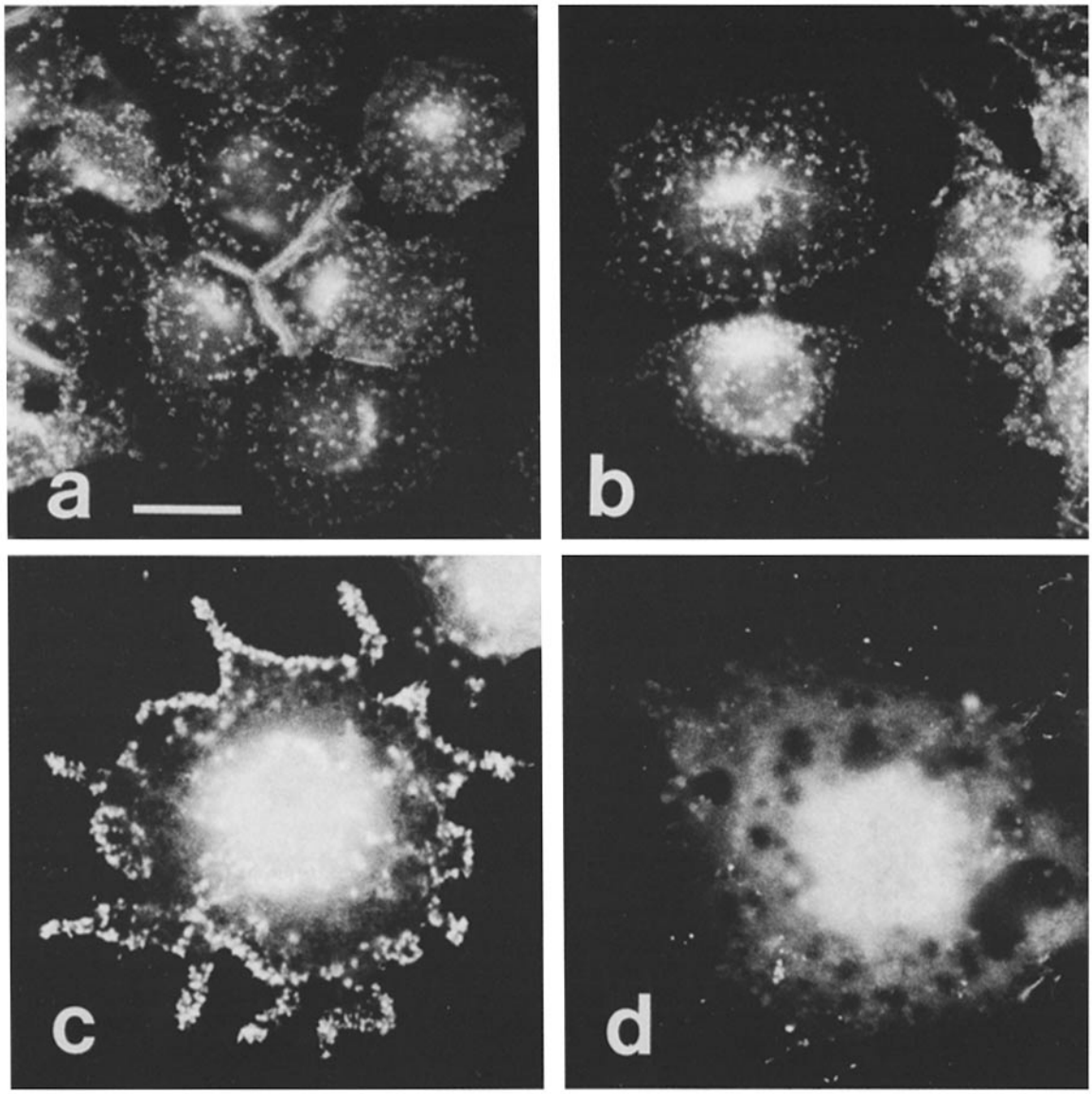

FIGURE 3 Fluorescent staining of adhesion plaques with antitumor serum is not diminished by preabsorption with unlabeled cytoskeletal proteins. SR-NRK cells were fixed and pp60^{src} stained by indirect immunofluorescence with antitumor serum either unabsorbed (*a*) or absorbed (*b*) with a myofibril extract from chicken gizzard (see Materials and Methods). In contrast, actin within the adhesion plaques of SR-NRK cells was stained with unabsorbed antiactin serum (*c*), but the staining was greatly diminished after absorption with the myofibril proteins (*d*). Bar, 20 μm.

in chick fibroblasts, which measure 0.1–2 μm wide by 2–10 μm long (23).

The composition of these isolated adhesion structures was investigated by challenging such preparations with antibodies against pp60^{src} and various cytoskeletal proteins (Fig. 5). Both adhesion plaques and junctions stained heavily as a result of antiactin (Fig. 5 *A*) or anti-α-actinin (Fig. 5 *B*) binding. The distribution of stain was quite similar to that observed at the ventral surface of fixed whole cells. Vinculin (Fig. 5 *C*) was localized in isolated adhesion junctions as a characteristic pattern of paired lines separated by a prominent gap, but very few adhesion plaques per se were visible after vinculin staining. By contrast, antitumor serum (Fig. 5 *D*) stained numerous "feet" as well as junctions. Anti-58,000-dalton antibody revealed that patches of intermediate filament protein remained nonspecifically associated with the adhesion plaque preparations, but no specific relationship with the adhesion structures was evident (Fig. 5 *E*). Tubulin was not found in these preparations (not shown).

Distribution of Actin, α-Actinin, Vinculin, and pp60^{src} within Isolated Intercellular Adhesion Junctions

Higher magnification views of isolated intercellular adhesion junctions stained with actin, α-actinin, vinculin, or pp60^{src} gave a clearer impression of the relative orientation of these proteins within the complex (Fig. 6). Actin and α-actinin were concentrated across the width of the junction (2–4 μm), except for a narrow gap of ~2,000 Å down the center. Vinculin stained only at the edges of the complex, resulting in an unstained region of ~1 μm across. pp60^{src} was present all across the junction, but appeared concentrated at the midline.

A scanning electron micrograph of an isolated adhesion

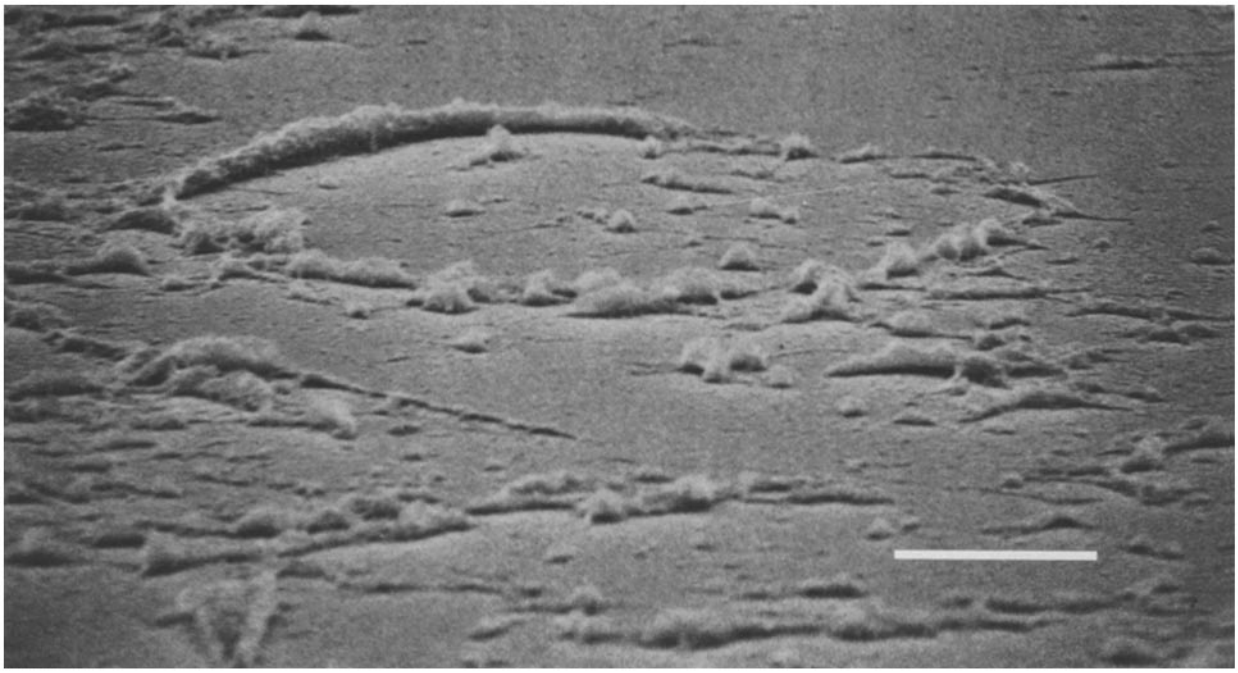

FIGURE 4 Scanning electron micrograph of isolated adhesion plaques. Adhesion plaques of SR-NRK cells were prepared as in Fig. 5. The isolated adhesion plaques were viewed at a 70° tilt in a Cambridge Stereoscan Mark II electron microscope. The adhesion plaques that outlined a single cell can be seen in the upper section of this photograph. Bar, 5 μm. × 2,600.

junction suggested an accumulation of fibrous material, bisected by a single cleft (Fig. 7). Although the photograph is distorted somewhat by a 25° tilt angle, it is apparent that the size of the cleft is roughly consistent with the gap observed by immunofluorescent staining of actin or α-actinin. The base of the adhesion junction revealed at the left side of the photograph exhibits a wider spacing that may be analogous to the paired lines of vinculin immunofluorescence which were characteristically observed.

DISCUSSION

The adhesion plaques presumably mediate adhesion of tissue culture cells to the surface on which they grow through transmembrane connections to the actin filaments. We have demonstrated (37) that $pp60^{src}$ is contained within the adhesion plaques of RSV-transformed cells and have developed techniques to isolate these structures still bound to the substratum. In addition to adhesion plaques, we have now characterized unique adhesive complexes that form at junctions between epithelioid SR-NRK cells. Our results demonstrate that the RSV *src* gene product ($pp60^{src}$) is associated with the cytoskeletal proteins actin, α-actinin, and vinculin at both adhesion plaques and junctions, and at the latter site a specific spatial organization of these proteins has been demonstrated. The coexistence of these proteins was shown by immunofluorescence both in whole fixed cells and in preparations of isolated adhesion structures. In contrast, microtubules and intermediate filaments were not associated with $pp60^{src}$ in the adhesion loci, although we cannot rule out the possibility that other types of intermediate filaments, not detected by the anti-58,000-dalton serum, may extend to these sites.

Of the three filamentous networks comprising the cellular cytoskeleton, only the stress fibers, composed of microfilament bundles, are overtly disrupted upon transformation by RSV (2, 12, 22, 31, 45). These stress fibers have been proposed as an early cytoplasmic target for the *src* gene product (2, 30, 45). In the SR-NRK cells used in our studies, stress fibers were not detectable and, instead of the diffuse distribution of actin reported in other RSV-transformed cells, punctate patches of actin were visible on the ventral cell surface corresponding to the adhesion plaques. An identical distribution of actin and α-actinin also was found using antisera produced and characterized in another laboratory,[1] and the distribution of actin was not changed by substituting an alternative method of fixation employing 1% glutaraldehyde followed by methanol (48). These results indicate that the dissolution of microfilament bundles and the redistribution of actin to adhesion plaque sites is a property of the epithelioid SR-NRK line and not artifactual.

In addition to adhesion plaques, the epithelioid line of SR-NRK cells described in this study exhibited unique complexes at cell-cell junctions. We previously demonstrated (36) that epithelioid clones of SR-NRK exhibit intense $pp60^{src}$ fluorescence at cell contacts, whereas the occurrence of such boundaries is less frequent in fibroblastic counterparts. These differences are likely related to the tendency of epithelioid cells to pack closely and form specialized junctional complexes (13). Several observations suggest that adhesion plaques may be related to these complex junctions that form between SR-NRK cells. Ultrastructural studies have noted marked similarities between the electron-dense areas underlying the cytoplasm of colliding fibroblasts at points of cell-cell contact and the areas of cell-substrate adhesion (9, 20). In normal cells, microfilaments are specifically associated with both types of specialized regions. Perhaps the most compelling observation is that both structures contain the same cytoskeletal proteins—actin, α-actinin, and vinculin. The presence of these proteins has been reported previously in clusters of adhesion plaques aligned

[1] L. Rohrschneider and K. Weber. Unpublished observations.

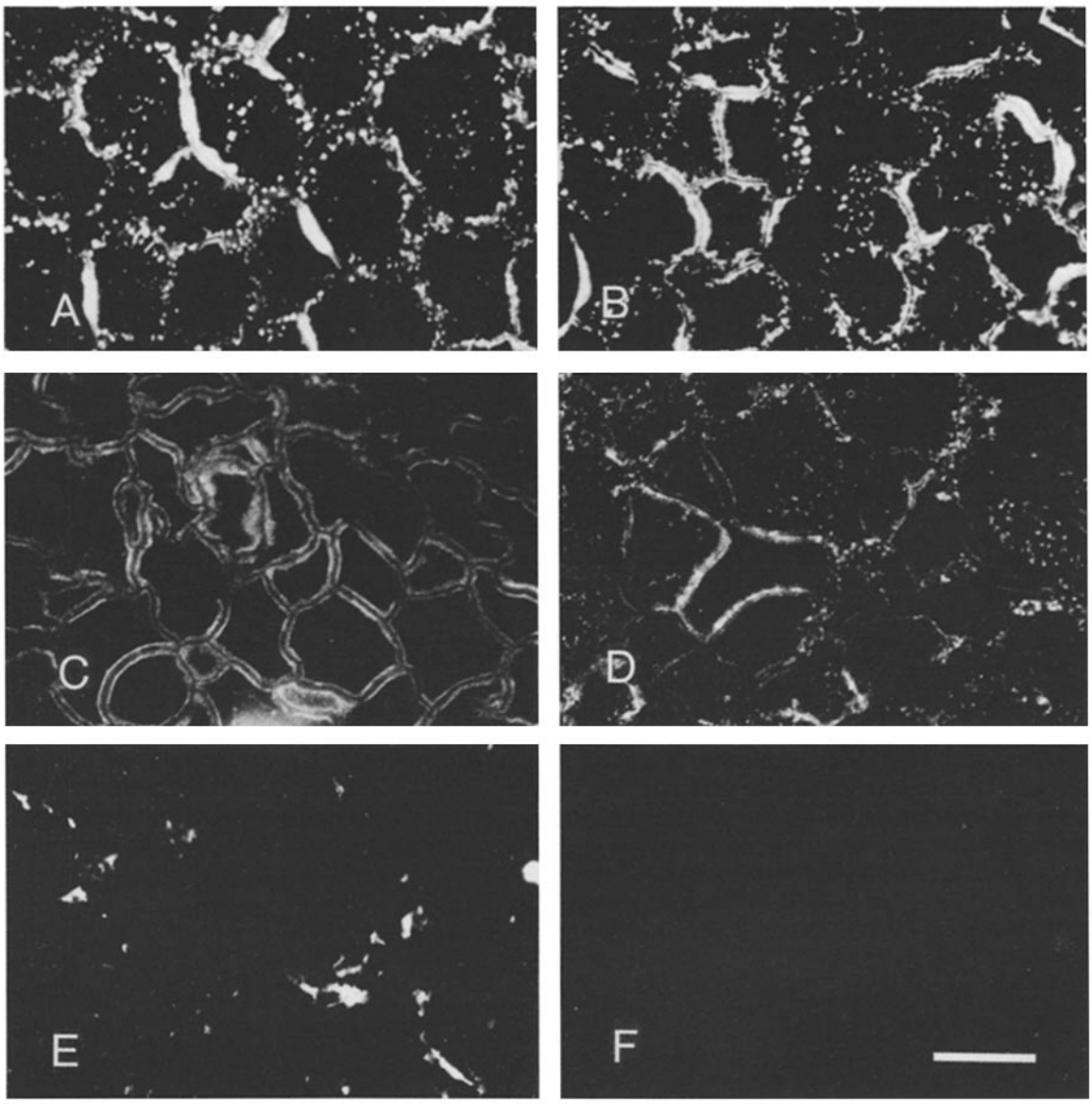

FIGURE 5 Immunofluorescent staining of actin, α-actinin, vinculin, pp60^{src}, and intermediate filament protein within isolated adhesion plaques. SR-NRK cells, grown on glass cover slips, were removed from the substratum under conditions that leave the adhesion plaques and adhesion junctions bound to the glass cover slips (see Materials and Methods). These structures were stained by indirect immunofluorescence using antisera to (*A*) actin, (*B*) α-actinin, (*C*) vinculin, (*D*) pp60^{src}, (*E*) the 58,000-dalton intermediate filament protein, and (*F*) normal rabbit serum. The speckled pattern of fluorescence is due to the adhesion plaque structures, whereas the solid lines of fluorescence correspond to the adhesive residue remaining at the junctions between cells. These structures are termed adhesion junctions. Bar, 20 μm.

between cells in contact (16, 27). In addition, pp60^{src} is contained within both adhesion plaques and junctions. Further studies are planned to evaluate the potential relationship between these structures.

We have exploited the morphological characteristics of epithelioid SR-NRK cells to examine a spatial organization of actin, α-actinin, vinculin, and pp60^{src} which is apparent in the adhesion junctions. This organization may exist in the adhesion plaques as well, but is not obvious because of their small size and perhaps orientation. At the adhesion junctions, pp60^{src} is concentrated at the midline. It seems unlikely that this pattern is caused by an accumulation of the transforming gene product within the intermembranal space between apposed cells, because pp60^{src} cannot be detected by immunofluorescence without permeabilizing the cells (35). Presumably, pp60^{src} is localized very close to the membrane on the cytoplasmic side of each cell, a site which is consistent with recent immunoferritin studies (50). An absence of fluorescence within the lipid bilayer and 100- to 200-Å intercellular gap would not be resolved by this technique, which has a calculated limit of resolution of ~2,000 Å (32). Actin and α-actinin are clearly excluded from the midline where pp60^{src} is most abundant but form heavy accumulations of material, which appear fibrous in scanning electron microscopic views, on the cytoplasmic side of pp60^{src}. In fact, actin is the major protein visible on SDS-polyacrylamide gels of isolated "feet" (not shown). The fine line of vinculin fluorescence appearing at the cytoplasmic edge of the junction could be interpreted several ways in theoretically reconstructing the structure. Vinculin may be bound along the whole inner edge of the actin/α-actinin aggregate on either

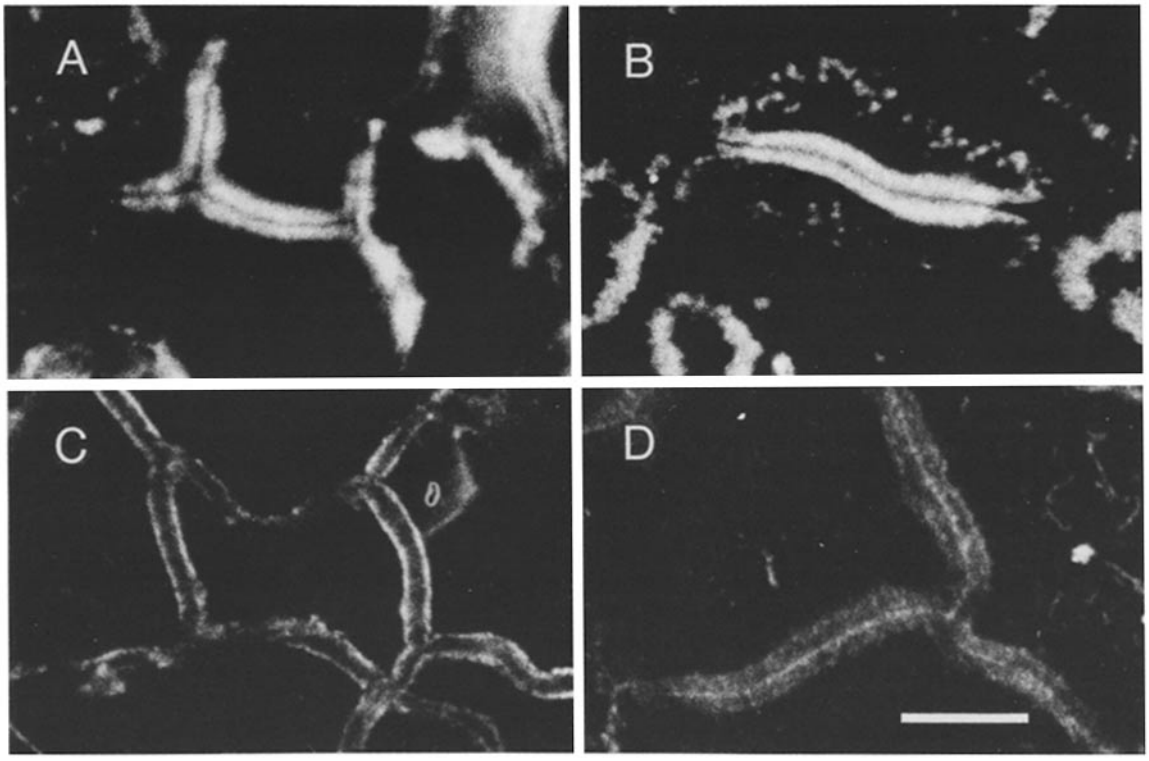

FIGURE 6 Detailed immunofluorescent staining of actin, α-actinin, vinculin, and pp60^{src} within isolated adhesion junctions of SR-NRK cells. SR-NRK cells were removed from the glass substratum on which they were growing, leaving behind the adhesion plaques and adhesion junctions. The cover slips were stained by indirect immunofluorescence with antisera to (*A*) actin, (*B*) α-actinin, (*C*) vinculin, and (*D*) pp60^{src}. Details of the stained adhesion junctions are shown in this figure. Bar, 10 μm.

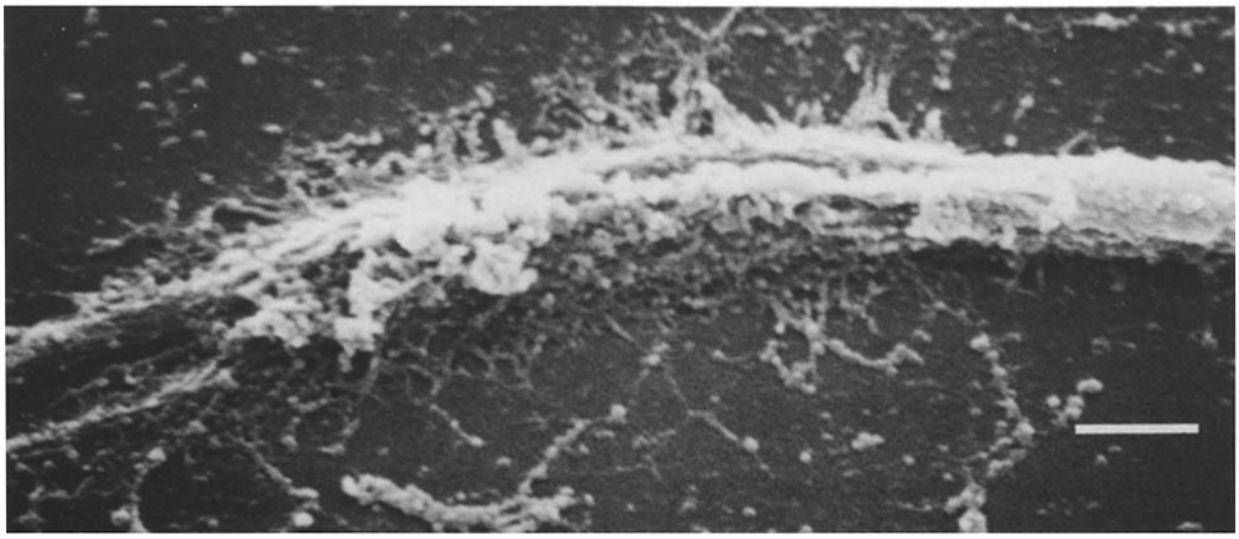

FIGURE 7 Scanning electron micrograph of an isolated adhesion junction. Isolated adhesion junctions of SR-NRK cells were prepared on glass cover slips. This figure shows a typical adhesion junction photographed with a Cambridge Stereoscan Mark II electron microscope at a 25° tilt. Compare this structure with the immunofluorescence data shown in Fig. 6. Bar, 1 μm. × 8,300.

side of the adhesion, or the pattern may result from vinculin located only at the base of the adhesion, where it is involved in the attachment of the adhesion junctions to the substratum. The latter model is attractive because it is consistent with the apparent affinity of this protein for juxtamembranal sites (17).

Another feature of interest is the distribution of vinculin within adhesion structures of sparse vs. confluent cultures. In sparse cultures of SR-NRK cells, many adhesion plaques with an accumulation of pp60^{src} were evident. Not all of these adhesion plaques, however, appeared to contain vinculin. This distinction appeared to be more pronounced in areas where cell-cell junctions had formed. When isolated adhesion plaques and junctions were prepared from confluent cultures, the junctions stained for vinculin as noted above, but virtually no staining of vinculin was observed in the adhesion plaques beneath these cells (see Fig. 5). Adhesion plaques existed under these confluent cells and were stainable with antisera to actin, α-actinin, and pp60^{src}. It is possible that vinculin was selectively

extracted from the adhesion plaques but not from the junctions during the isolation procedure. But our observations in whole cells suggest either that vinculin redistributes to the adhesion junctions during cell-cell contact or, alternatively, that the action of pp60^{src} within the adhesion plaques leads to the displacement of vinculin.

The *src* gene product within the adhesion plaques and adhesion junctions was not extractable by buffers containing nonionic detergents (see Materials and Methods). The insoluble nature of pp60^{src} within these structures suggests that it is not simply an integral membrane protein bound to the plasma membrane through hydrophobic interactions at these sites. Rather, it is more plausible that pp60^{src} acquires this property of insolubility through direct interaction with components of the insoluble cytoskeleton. At other plasma membrane sites, pp60^{src} has been described as an integral membrane protein (10, 26). However, it should be considered that pp60^{src} also could interact with cytoskeletal elements subjacent to the plasma membrane.

Transformation by RSV most likely proceeds through pp60^{src}-mediated phosphorylations of host cell proteins on tyrosine amino acids (8, 40). It is intriguing to speculate that disruption of the cytoskeletal network in transformed cells could occur as a result of phosphorylation of one or more proteins essential in linking this network to the membrane at the adhesion plaque sites. Vinculin may be such a linkage protein (7, 16, 17). In this respect, we have identified by immunoprecipitation both vinculin and pp60^{src} as proteins specifically phosphorylated after incubation of isolated SR-NRK feet with [γ-^{32}P]ATP (42). Vinculin, therefore, may be a substrate protein for pp60^{src} within the adhesion plaques. We are now investigating whether this interaction is necessary and/or sufficient for oncogenic transformation.

We thank Paul Neiman and Breck Byers for critical evaluation of the manuscript and Bob Ramberg for use of the fluorescence microscope.

This work was supported by National Cancer Institute grants CA 20551 and CA 09229.

Received for publication 1 December 1980, and in revised form 29 January 1981.

REFERENCES

1. Abercrombie, M., and G. A. Dunn. 1975. Adhesions of fibroblasts to substratum during contact inhibition observed by interference reflection microscopy. *Exp. Cell Res.* 92:57–62.
2. Ash, J. F., P. K. Vogt, and S. J. Singer. 1976. Reversion from transformed to normal phenotype by inhibition of protein synthesis in rat kidney cells infected with a temperature-sensitive mutant of Rous sarcoma virus. *Proc. Natl. Acad. Sci. U. S. A.* 73:3603–3607.
3. Brugge, J. S., and R. L. Erikson. 1977. Identification of a transformation-specific antigen induced by an avian sarcoma virus. *Nature (Lond.).* 269:346–348.
4. Brugge, J. S., P. J. Steinbaugh, and R. L. Erikson. 1978. Characterization of the avian sarcoma virus protein p60^{src}. *Virology.* 91:130–140.
5. Brugge, J. S., M. S. Collett, A. Siddiqui, B. Marczynska, F. Deinhardt, and R. L. Erikson. 1979. Detection of the viral sarcoma gene product in cells infected with various strains of avian sarcoma virus and of a related protein in uninfected chicken cells. *J. Virol.* 29:1196–1203.
6. Burr, J. G., G. Dreyfuss, S. Penman, and J. M. Buchanan. 1980. Association of the *src* gene product of Rous sarcoma virus with cytoskeletal structures of chicken embryo fibroblasts. *Proc. Natl. Acad. Sci. U. S. A.* 77:3484–3488.
7. Burridge, K., and J. R. Feramisco. 1980. Microinjection and localization of a 130K protein in living fibroblasts: a relationship to actin and fibronectin. *Cell.* 19:587–595.
8. Collett, M. S., and R. L. Erikson. 1978. Protein kinase activity associated with the avian sarcoma virus *src* gene product. *Proc. Natl. Acad. Sci. U. S. A.* 75:2021–2024.
9. Cornell, R. 1969. Cell-substrate adhesion during cell culture. An ultrastructural study. *Exp. Cell Res.* 58:289–295.
10. Courtneidge, S. A., A. D. Levinson, and J. M. Bishop. 1980. The protein encoded by the transforming gene of avian sarcoma virus (pp60^{src}) and a homologous protein in normal cells (pp60$^{proto\text{-}src}$) are associated with the plasma membrane. *Proc. Natl. Acad. Sci. U. S. A.* 77:3783–3787.
11. Curtis, A. S. G. 1964. The mechanism of adhesion of cells to glass. *J. Cell Biol.* 20:199–215.
12. Edelman, G. M., and J. Yahara. 1976. Temperature sensitive changes in surface modulating assemblies of fibroblasts transformed by mutants of Rous sarcoma virus. *Proc. Natl. Acad. Sci. U. S. A.* 73:2047–2051.
13. Farquhar, M. G., and G. E. Palade. 1963. Junctional complexes in various epithelia. *J. Cell Biol.* 17:375–412.
14. Franke, W. W., E. Schmid, M. Osborn, and K. Weber. 1978. Different intermediate-sized filaments distinguished by immunofluorescence microscopy. *Proc. Natl. Acad. Sci. U. S. A.* 75:5034–5038.
15. Fuller, G. M., B. R. Brinkley, and J. M. Broughter. 1975. Immunofluorescence of mitotic spindles by using monospecific antibody against bovine brain tubulin. *Science (Wash. D. C.).* 187:948–950.
16. Geiger, B. 1979. A 130K protein from chicken gizzard: its localization at the termini of microfilament bundles in cultured chicken cells. *Cell.* 18:193–205.
17. Geiger, B., K. T. Tokuyasu, A. H. Dutton, and S. J. Singer. 1980. Vinculin, an intracellular protein localized at specialized sites where microfilament bundles terminate at cell membranes. *Proc. Natl. Acad. Sci. U. S. A.* 77:4127–4131.
18. Gordon, W. E., A. Bushnell, and K. Burridge. 1978. Characterization of the intermediate (10 nm) filaments of cultured cells using an autoimmune rabbit antiserum. *Cell.* 13:249–261.
19. Heath, V. P., and G. A. Dunn. 1978. Cell to substratum contacts of chick fibroblasts and their relation to the microfilament system. A correlated interference-reflexion and high-voltage electron-microscope study. *J. Cell Sci.* 29:197–212.
20. Heaysman, J. E. M., and S. M. Pegrum. 1973. Early contacts between fibroblasts: an ultrastructural study. *Exp. Cell Res.* 78:71–78.
21. Hunter, T., and B. M. Sefton. 1980. The transforming gene product of Rous sarcoma virus phosphorylates tyrosine. *Proc. Natl. Acad. Sci. U. S. A.* 77:1311–1315.
22. Hynes, R. O., and A. T. Destree. 1978. 10 nm filaments in normal and transformed cells. *Cell.* 13:151–163.
23. Izzard, C. S., and L. R. Lochner. 1976. Cell-to-substrate contacts in living fibroblasts: an interference reflexion study with an evaluation of the technique. *J. Cell Sci.* 21:129–159.
24. Karsenti, E., B. Guilbert, M. Bornens, and S. Avrameas. 1977. Antibodies to tubulin in normal nonimmunized animals. *Proc. Natl. Acad. Sci. U. S. A.* 74:3997–4001.
25. Krueger, J. G., E. Wang, and A. R. Goldberg. 1980. Evidence that the *src* gene product of Rous sarcoma virus is membrane associated. *Virology.* 101:25–40.
26. Krueger, J. G., E. Wang, E. A. Garber, and A. R. Goldberg. 1980. Differences in intracellular location of pp60^{src} in rat and chicken cells transformed by Rous sarcoma virus. *Proc. Natl. Acad. Sci. U. S. A.* 77:4142–4146.
27. Lazarides, E., and K. Burridge. 1975. α-Actinin: immunofluorescent localization of a muscle structural protein in nonmuscle cells. *Cell.* 6:289–298.
28. Lazarides, E., and K. Weber. 1974. Actin antibody: the specific visualization of actin filaments in non-muscle cells. *Proc. Natl. Acad. Sci. U. S. A.* 71:2268–2272.
29. Levinson, A. D., H. Oppermann, L. Levintow, H. E. Varmus, and J. M. Bishop. 1978. Evidence that the transforming gene of avian sarcoma virus encodes a protein kinase associated with a phosphoprotein. *Cell.* 15:561–572.
30. McClain, D. A., P. F. Maness, and G. M. Edelman. 1978. Assay for early cytoplasmic effects of the *src* gene product of Rous sarcoma virus. *Proc. Natl. Acad. Sci. U. S. A.* 75:2750–2754.
31. Osborn, M., and K. Weber. 1977. The display of microtubules in transformed cells. *Cell.* 12:561–571.
32. Osborn, M., R. E. Webster, and K. Weber. 1978. Individual microtubules viewed by immunofluorescence and electron microscopy in the same PtK2 cell. *J. Cell Biol.* 77:R27–R34.
33. Pope, J. H., and W. P. Rowe. 1964. Detection of specific antigens in SV40 transformed cells by immunofluorescence. *J. Exp. Med.* 120:121–128.
34. Purchio, A. F., E. Erikson, J. S. Brugge, and R. L. Erikson. 1978. Identification of a polypeptide encoded by the avian sarcoma virus *src* gene. *Proc. Natl. Acad. Sci. U. S. A.* 75:1567–1571.
35. Rohrschneider, L. R. 1979. Immunofluorescence on avian sarcoma virus-transformed cells: localization of the *src* gene product. *Cell.* 16:11–24.
36. Rohrschneider, L. R. 1979. Localization of pp60^{src} within NRK cells infected with temperature-sensitive mutants (T class) of Rous sarcoma virus. *Cold Spring Harbor Symp. Quant. Biol.* 44:1013–1021.
37. Rohrschneider, L. R. 1980. Adhesion plaques of Rous sarcoma virus-transformed cells contain the *src* gene product. *Proc. Natl. Acad. Sci. U. S. A.* 77:3514–3518.
38. Rohrschneider, L. R., R. N. Eisenman, and C. R. Leitch. 1979. Identification of a Rous sarcoma virus transformation-related protein in normal avian and mammalian cells. *Proc. Natl. Acad. Sci. U. S. A.* 76:4479–4483.
39. Sefton, B. M., K. Beemon, and T. Hunter. 1978. Comparison of the *src* gene of Rous sarcoma virus *in vitro* and *in vivo*. *J. Virol.* 28:957–971.
40. Sefton, B. M., T. Hunter, K. Beemon, and W. Eckhart. 1980. Evidence that the phosphorylation of tyrosine is essential for cellular transformation by Rous sarcoma virus. *Cell.* 20:807–816.
41. Shelanski, M. L., F. Gaskin, and C. R. Cantor. 1973. Microtubule assembly in the absence of added nucleotides. *Proc. Natl. Acad. Sci. U. S. A.* 70:765–768.
42. Shriver, K., and L. Rohrschneider. 1980. Spatial and enzymatic interaction of pp60^{src} with cytoskeletal proteins in isolated adhesion plaques and junctions from RSV-transformed NRK cells. *Cold Spring Harbor Conf. Cell Proliferation.* 8: In press.
43. Singh, I., D. E. Goll, R. M. Robson, and M. H. Stromer. 1977. N- and C-terminal amino acids of purified α-actinin. *Biochim. Biophys. Acta.* 491:29–45.
44. Ternynck, T., and S. Avrameas. 1976. Polymerization and immobilization of proteins using ethylchloroformate and glutaraldehyde. *Scand. J. Immunol. Suppl.* 3:29–35.
45. Wang, E., and A. R. Goldberg. 1976. Changes in microfilament organization and surface topography upon transformation of chick embryo fibroblasts with Rous sarcoma virus. *Proc. Natl. Acad. Sci. U. S. A.* 73:4065–4069.
46. Wang, L.-H. 1978. The gene order of avian RNA tumor viruses derived from biochemical analyses of deletion mutants and viral recombinants. *Annu. Rev. Microbiol.* 32:561–592.
47. Weber, K., R. Pollack, and T. Bibring. 1975. Antibody against tubulin: the specific visualization of cytoplasmic microtubules in tissue culture cells. Proc. Natl. Acad. Sci. U. S. A. 72:459–463.
48. Weber, K., P. C. Rathke, and M. Osborn. 1978. Cytoplasmic microtubular images in glutaraldehyde-fixed tissue culture cells by electron microscopy and by immunofluorescence microscopy. *Proc. Natl. Acad. Sci. U. S. A.* 75:1820–1824.
49. Weisenberg, R. C. 1972. Microtubule formation *in vitro* in solutions containing low calcium concentration. *Science (Wash. D. C.).* 177:1104–1105.
50. Willingham, M. C., G. Jay, and I. Pastan. 1979. Localization of the avian sarcoma virus *src* gene product to the plasma membrane of transformed cells by electron microscopic immunocytochemistry. *Cell.* 18:125–134.
51. Witman, G. B., D. W. Cleveland, M. D. Weingarten, and M. W. Kirschner. 1976. Tubulin requires tau for growth onto microtubule initiating sites. *Proc. Natl. Acad. Sci. U. S. A.* 73:4070–4074.